Pergamon

Int. J. Mach. Tools Manufact. Vol. 36, No. 3, pp. 307–323, 1996
Elsevier Science Ltd
Printed in Great Britain
0890–6955/96$15.00 + .00

0890–6955(95)00069-0

THREE-DIMENSIONAL CUTTING FORCE ANALYSIS BASED ON THE LOWER BOUNDARY OF THE SHEAR ZONE. PART 1: SINGLE EDGE OBLIQUE CUTTING

PATRI K. VENUVINOD† and W. L. JIN‡

(*Received* 18 *January* 1995; *in final form* 10 *July* 1995)

Abstract—Traditional models of cutting based on Merchant's shear plane idealization are incapable of predicting any of the cutting force components without *a priori* knowledge of chip–tool friction. However, Rubenstein's work on orthogonal cutting has shown that this limitation can be avoided by utilizing the stress distributions on the lower boundary of the shear zone. The present work aims to extend this approach to oblique cutting with single and two edged tools. This paper focuses on single edge oblique cutting whereas Part 2 analyses two edge cutting. It is assumed that the progressive deformation of the work material into chip material occurs within the effective plane. The resulting stress distributions on the lower boundary are integrated to yield expressions for estimating cutting forces from given tool and chip geometries. This provides a mechanism for predicting the power and lateral components of the cutting force in single edge oblique cutting. The predictions are verified against new and previously published experimental data.

NOMENCLATURE

A_m	area of "Merchant" shear plane
$\mathbf{A}_m$	area vector of Merchant shear plane, i.e. vector with magnitude equal to A_m and directed perpendicular to P_m (directed towards chip material)
b	workpiece width
C	a constant related to the normal stress distribution on the true lower boundary of the shear zone (TLB) (equal to p/p_w)
dA	an area element on the TLB
$\mathbf{dA}$	area vector of dA, i.e. a vector with magnitude equal to the area of dA and directed normal to dA and directed towards the chip material
df_j	contribution to f_j due to deformation at dA
f_{cd}	cutting force component parallel to the cutting edge
f_j	cutting force vector in direction j
f_P	cutting force component in the direction of $\mathbf{V}$
f_{Pn}	cutting force component parallel to P_s and perpendicular to the cutting edge
f_Q	cutting force component perpendicular to P_s
f_R	cutting force component perpendicular to f_P and f_Q
p	mean normal stress on the segment of the TLB which is not parallel to P_s
p_{dA}	normal stress on dA
p_w	normal stress on the TLB where the TLB meets the unmachined work surface
p_m	mean normal stress on the segment of the TLB which is parallel to P_s
P_d	plane in which the progressive deformation of an element of work material into the corresponding chip element is assumed to occur
P_{ef}	the effective plane, plane parallel to $\mathbf{V}$ and $\mathbf{V}_c$
P_m	plane passing through the Merchant shear plane, i.e. the plane passing through the cutting edge and the line of intersection between the initial work surface and the chip surface
P_n	"normal" plane, i.e. the plane perpendicular to the cutting edge
P_s	tool cutting edge plane, i.e. the plane containing the cutting edge and $\mathbf{V}$
s	shear flow stress of unmachined work material (a work material property)
t	undeformed chip thickness
$\mathbf{u}_{ndA}$	unit vector normal to dA (directed towards chip material)
$\mathbf{u}_{nd}$	unit vector perpendicular to P_d
$\mathbf{u}_{nef}$	unit vector perpendicular to P_{ef}
$\mathbf{u}_j$	unit vector parallel to an arbitrary direction j
$\mathbf{u}_{nm}$	unit vector perpendicular to P_m (directed towards chip material)
$\mathbf{u}_{V_s}$	unit vector parallel to $\mathbf{V}_s$
V,$\mathbf{V}$	magnitude of cutting velocity and cutting velocity vector (directed towards the cutting edge), respectively

†Department of Manufacturing Engineering, City University of Hong Kong, Hong Kong.
‡Nanjing University of Aeronautics and Astronautics, Nanjing, People's Republic of China.

V_c,$\mathbf{V}_c$	magnitude of chip velocity and chip velocity vector (directed away from the cutting edge), respectively
V_s,$\mathbf{V}_s$	magnitude of shear velocity and shear velocity vector P_m; ($\mathbf{V}_s = \mathbf{V} - \mathbf{V}_c$)
V_x,V_y,V_z	velocity components of a material element parallel to axes x, y and z, respectively
γ_n	"normal" rake angle, i.e. the rake angle measured in P_n
$\dot{\epsilon}_x$, $\dot{\epsilon}_y$, $\dot{\epsilon}_z$	strain rates in the directions of axes x, y and z, respectively
$\dot{\epsilon}_{xy}$, $\dot{\epsilon}_{yz}$, $\dot{\epsilon}_{xz}$	shear strain rates on area elements parallel to planes xy, yz, and xz, respectively
η_c	chip flow angle, i.e. the angle between $\mathbf{V}_c$ and the line of intersection between the rake face and P_n
η_s	acute angle between the shear velocity at a point along the TLB and P_n when measured in the plane tangent to TLB
η_{sw}	magnitude of η_s at the junction between chip surface and the unmachined work surface
η_{sw}^{ef}	the magnitude of η_{sw} when $P_d \equiv P_{ef}$
η_{sm}	acute angle between $\mathbf{V}_s$ and the line of intersection between P_m and P_n
λ_s	angle of inclination of the cutting edge, i.e. the acute angle between $\mathbf{V}$ and P_n
ξ_{dA}	acute angle between $\mathbf{u}_{ndA}$ and $\mathbf{u}_{nd}$ (or $\mathbf{u}_{nef}$)
ξ_a,ξ_2	magnitudes of ξ_{dA} for planes 1 and 2, respectively, in Fig. 2(b)
σ_m	mean normal stress in a material element
σ_x,σ_y,σ_z	normal stresses on area elements perpendicular to axes x, y and z, respectively
σ_θ	normal stress on an area element perpendicular to the yz plane and inclined at angle θ to plane xy as shown inFig. 4
τ_s	mean shear stress on the Merchant shear plane, P_m
τ_{xy}, τ_{yz}, τ_{xz}	shear stresses on area elements parallel to planes xy, yz, and xz, respectively
$\tau_{y\theta}$	shear stress on a plane parallel to axis x and inclined at angle θ to the xy plane
ϕ_n	"normal" shear angle, i.e. the acute angle between P_m and P_s
ϕ_e	"effective" shear angle, i.e. the acute angle between $\mathbf{V}$ and $\mathbf{V}_s$
ψ_n	acute angle between the plane tangential to the TLB (at a given point) and P_s
ψ_{nw}	magnitude of ψ_n at the junction between chip and unmachined work surfaces

1. INTRODUCTION

Given the practical importance of metal cutting, it is essential to acquire a deep understanding of the cutting process through models which stand up to experimental verification. In order to be useful, these models must be able to predict machining variables of practical importance (such as cutting forces, cutting temperatures, and tool wear rates) in addition to providing as accurate an understanding as possible of what goes on in the machining process.

Although cutting tools with complex chip formers are being increasingly used to provide a degree of chip control, the majority of cutting tools continue to utilize cutting wedges formed by plane faces. The cutting edges in these tools are straight. Figure 1

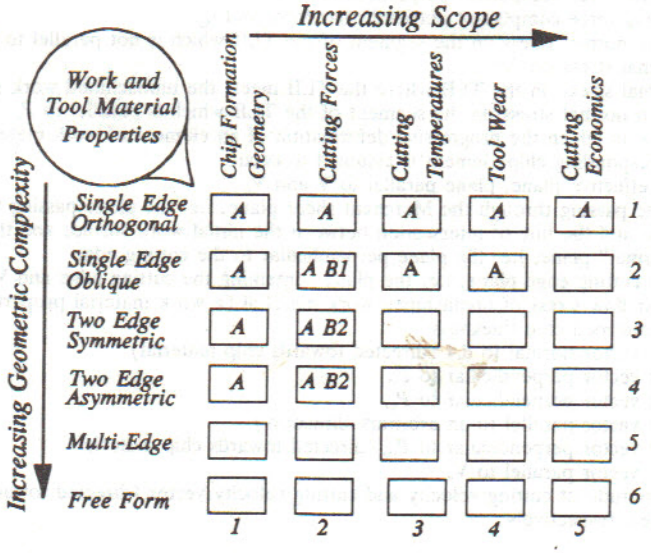

A: Significant publications available
B1: Subjects of part Part I and Part II respectively of the present study

Fig. 1. Modelling tasks in cutting with plane faced cutting wedges.

provides an overview of the tasks involved in the modelling of machining operations with such tools. These tasks are ordered along the horizontal axis in terms of increasing range of the machining variables to be predicted and, along the vertical axis, in terms of increasing geometrical complexity. Thus, "cutting forces" is placed at a higher level than "chip formation" along the horizontal axis since the former includes, by its very nature, a consideration of the latter. Likewise, single edge orthogonal cutting is placed at a lower level on the vertical axis than oblique cutting since the former is the special case of the latter occurring when the angle of inclination, λ_s, of the cutting edge is equal to zero. It follows from the ordering of these tasks that progress in modelling metal cutting should typically start from task (1,1) and proceed towards task (6,5). A review of the historical trends in metal cutting modelling generally confirms this observation.

The ultimate goal is to be able to model task (6,5) (i.e. economics of cutting with form tools) purely on the basis of tool and work material properties and the general principles of mechanics, heat transfer, tribology, and economics. However, despite numerous research efforts, even task (1,1), i.e. the task of predicting the geometry of chip formation in orthogonal cutting solely on the basis of given tool and work material properties, has not been satisfactorily resolved so far. This is partly because the strains, strain rates and temperatures associated with metal cutting are far removed in magnitude from those associated with basic material tests such as the tension test. Consequently, some researchers now believe that it is more fruitful to consider single edge cutting as a material test in its own right and use the results thus obtained as the basis for modelling tasks at higher levels. The present work is based on this premise. Interestingly, a review of the literature based on this premise indicates that reasonably satisfactory models exist only for the tasks marked A in Fig. 1. The overall aim of the present work is to be able to model the next logical task, i.e. task (4,2): two edge asymmetric cutting, in a manner consistent with the modelling of cutting forces in single edge orthogonal cutting. Further, the model should be able to predict the cutting forces arising from individual cutting edges, i.e. it should be able to partition the overall cutting force components between the two participating cutting edges. It may be noted that further progress beyond task (4,2) is not possible unless this force partitioning problem is solved. This is because the partitioned forces determine the thermal energy generated at each cutting edge which, in turn, will determine the temperature distribution and wear rate at the edge. This paper addresses tasks marked B1 whereas tasks marked B2 are addressed in Part 2.

Amongst the various approaches used in modelling cutting forces, the shear plane approach, originally developed by Merchant [1], stands out as the most extensively applied. In this approacch, the chip is considered to be a rigid body in translational equilibrium under the action of the external forces acting on it. (Henceforth, this will be referred to as the Principle of Chip Equilibrium.) In the case of cutting with perfectly sharp single edge orthogonal tools, i.e. task (1,2), these external forces (i) lie in a plane orthgonal to the cutting edge, and (ii) act at the chip–tool interface, i.e. the shear plane, and the chip–tool interface, that is, the rake face. Subsequently, the shear plane approach was extended to single edge oblique cutting [1, 2]. As a result, each cutting force component could be described as a function of the cutting conditions (workpiece width being cut, b, and uncut chip thickness, t), the tool geometry (λ_s, and the normal rake angle, γ_n), the chip formation geometry (normal shear angle, ϕ_n, and chip flow angle, η_c), the shear flow strength of the work material at the shear plane, τ_s, and the apparent coefficient of friction at the chip–tool interface. However, the derivation of these functions required the additional application of the Principle of Force–Velocity Collinearity which assumes that the shear force, along the shear plane and the friction force, at the rake plane are collinear with the shear velocity, V_s, at the shear plane, and the chip velocity, V_c, relative to the tool, respectively.

Notwithstanding its widespread application, the best that can be said about Merchant's shear plane approach is that it provides a simple and elegant way of analysing a given

set of measured cutting forces. In particular, the Principle of Chip Equilibrium has stood the test of time. However, this approach does not have the ability to predict the magnitude of *any* of the cutting force components purely from a knowledge of chip formation geometry (i.e. ϕ_n and η_c) for given cutting conditions and tool geometry, i.e. its *predictive power* with regard to cutting force magnitudes is zero. This is because the prediction requires prior knowledge of the magnitude of the apparent coefficient of friction at the chip–tool interface which, in turn, is an entity related to cutting forces. Secondly, the magnitude of τ_s cannot be known *a priori* since it is the shear strength of the work material at the shear plane. The problem is that the shear plane is located somewhere in the middle of the shear zone (see Fig. 2) and one has no way of knowing, in practice, the magnitudes of the strains, strain rates, and temperatures prevailing in its vicinity. Clearly, the magnitudes of these strains, etc. must influence the magnitude of τ_s. A review of literature on the mechanics of metal cutting points to at least one alternative approach which is free from the limitations of the shear plane approach described above. This is the analysis based on the lower boundary of the shear zone as developed by Connolly and Rubenstein [3], and Rubenstein [4] for single edge orthogonal cutting. This model resulted in an estimate of the power component, f_P, of the cutting force purely in terms of the uncut area, ϕ_n, and the shear flow strength, s, of the unmachined work material. Extensive empirical evidence is available in support of this theory [3]. This means that, unlike the shear plane approach, Rubenstein's approach does not require *a priori* knowledge of the state of friction at the chip–tool interface. Thus, in contrast to Merchant's shear plane approach which has a predictive power of zero with regard to cutting forces, Rubenstein's approach has a predictive power equal to $\frac{1}{2}$, i.e. it can predict the magnitude of one of the two orthogonal force components.

To date, there has been only one attempt at extending Rubenstein's orthogonal cutting model to the case of single edge oblique cutting [5]. However, this work lacked rigour since it relied only on an intuitive definition of the stress distribution on the lower boundary of the shear zone. Subsequently, Lau and Rubenstein [6] and Rubenstein [7] proposed the concept of equivalent orthogonal cutting in order to enable the utilization of Rubenstein's orthogonal cutting solution based on the lower boundary of the shear zone [3, 4] in the modelling of oblique cutting. However, this model did not recognize the three-dimensional nature of the velocities and forces associated with the lower boundary of the shear zone in oblique cutting itself.

The objective of the present work is to develop a model of cutting forces based on

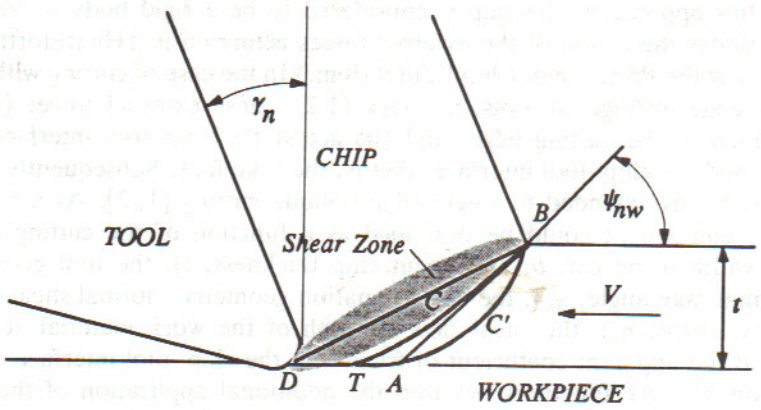

Fig. 2. The lower boundary of the shear zone in single edge orthogonal cutting.

a consideration of the lower boundary of the shear zone in oblique cutting which is in agreement with empirical evidence obtainned from single edge orthogonal cutting, single edge oblique cutting, two edge symmetric cutting and two edge oblique cutting, i.e. which is consistent across tasks (1,2)–(4,2) in Fig. 1. This paper describes a new model for single edge oblique cutting with a predictive power of at least $\frac{2}{3}$ with regard to cutting forces. (The model will be extended to the case of two edge oblique cutting in Part 2.)

2. THE LOWER BOUNDARY OF THE SHEAR ZONE IN SINGLE EDGE ORTHOGONAL CUTTING

Consider Fig. 2 which illustrates Rubenstein's model of orthogonal cutting [4]. Curve DTCB represents the true lower boundary (TLB) of the shear zone, whereas DB represents the Merchant shear plane. Basing his arguments on the plasticity conditions near the junction, B, between the TLB and the unmachined work surface, Rubenstein noted that the TLB must meet the unmachined work surface (at B) at 45° (i.e. $\psi_{nw} = 45°$) and the normal stress on the TLB should be uniformly distributed equal to the shear flow strength, s, of the unmachined work material. Likewise, on the basis of empirical evidence concerning chip–work material separation, he assumed that the TLB is parallel to the tool cutting edge plane, P_s, in the vicnity of D. Further, following a rigorous application of the translational equilibrium criterion to the tool–chip–shear-zone–workpiece system, Rubenstein made the following observations: "Provided the stresses (normal stress, p, and shear stress, s) are uniformly distributed, the force components f_P (parallel to the cutting speed) and f_Q (normal to the machined surface) are *path independent*, i.e. along any boundary joining B and D, including the Merchant shear plane, the same force components will be obtained when the magnitudes of the stresses (p and s) are specified. Of the infinity of paths joining B and D, one of these is the TLB. The force components acting on the TLB may be determined by calculating the force components along an arbitrarily chosen boundary joining the extremities of the TLB provided (i) the stresses which are assumed to act on the arbitrarily chosen boundary are the same as those acting on the TLB, and (ii) the stresses are uniformly distributed" [4].

Rubenstein next observed that if the assumed boundary (DTC'B) had a segment (TD) coincident with the TLB (DTCB) and the TLB is subjected, in its non-coincident segment (TCB), to uniformly distributed stresses, the force components calculated by integrating over the assumed boundary will be the same as those calculated by integrating over the entire TLB, irrespective of whether or not the assumed boundary has any physical significance [4].

Based on this premise, Rubenstein chose an assumed boundary represented by planes DA and AB which are tangential to the TLB at the latter's extremities D and B, respectively. Following the above arguments: (i) the shear stress on DA and AB were taken to be uniformly distributed with its magnitude equal to s; (ii) the normal stress, p, on AB was taken to be uniformly distributed and equal in magnitude to the shear stress, s; and (iii) the normal stress on DA was taken to be of unknown distribution and magnitude. Integration of these stresses over path DAB yielded the following equation for estimating f_P which is a function of just s, the uncut area (equal to $b\,t$), and the shear angle, ϕ_n:

$$f_P = s\,b\,t(\cot\phi_n + 1)\,. \tag{1}$$

This equation has been shown to be quite accurate and robust in the light of extensive experimental data obtained from orthogonal cutting [3].

3. ASSUMPTIONS

The following assumptions have been made in extending Rubenstein's single edge orthogonal cutting model [4] to single edge oblique cutting:

A1. The cutting tool is perfectly sharp.
A2. The work material is a perfectly plastic and isotropic continuum (by definition, the work material at the lower boundary has experienced no work hardening due to cutting).
A3. Chip formation is of type 2 (continuous chip with no built up edge present).
A4. The Principle of Chip Equilibrium is obeyed, i.e. the chip may be considered as a rigid body in translational equilibrium under the action of the forces exerted on it from the shear zone and the chip/tool interface at the tool rake face.
A5. The nature of chip deformation is identical at any location along the active cutting edge.
A6. The primary deformation shear zone is thin, i.e. its thickness is substantially smaller than its length.
A7. The progressive deformation of an element of work material into the corresponding element in the chip material occurs within a plane. (We will call the deformation plane P_d. The orientation of P_d is unknown at this stage of the analysis. However, further analysis will be directed towards identifying this plane.)

4. THE TLB IN OBLIQUE CUTTING

Consider how the basic notions contained in Rubenstein's model of TLB in orthogonal cutting [4] may be extended to single edge oblique cutting. Figure 3(a) illustrates the proposed approach. D′D″ is the active cutting edge. B′B″ is the intersection between the chip surface and the unmachined work surface. Plane B′B″D″D′ is the Merchant shear plane. The TLB is a curved surface joining B′B″ and D′D″. As in [4], the TLB is assumed to be tangential to the cutting plane, P_s, in the vicinity of the cutting edge and to meet the unmachined work surface at the other end, B′B″, at angle ψ_{nw} when measured in the normal plane, P_n. Thus, while segment D′D″T″T′ of the TLB is parallel to the cutting plane, P_s, the exact geometry of the non-coincident segment, B′B″T″T′, remains unknown.

Consider an area element of area dA located on the TLB [see Fig. 3(a)]. Let $\mathbf{u}_{ndA}$ be the unit vector normal to the area element. As in [4], it will be assumed that the shear stress is the same at every location on the TLB and has its magnitude equal to the shear flow strength, s, of the unmachined work material. However, unlike in [4], it is recognized that the normal stress could be distributed non-uniformly over the TLB. Let p_{dA} be the normal stress on dA so that $p_{dA}\,(dA)\,\mathbf{u}_{ndA}$ is the vector representing

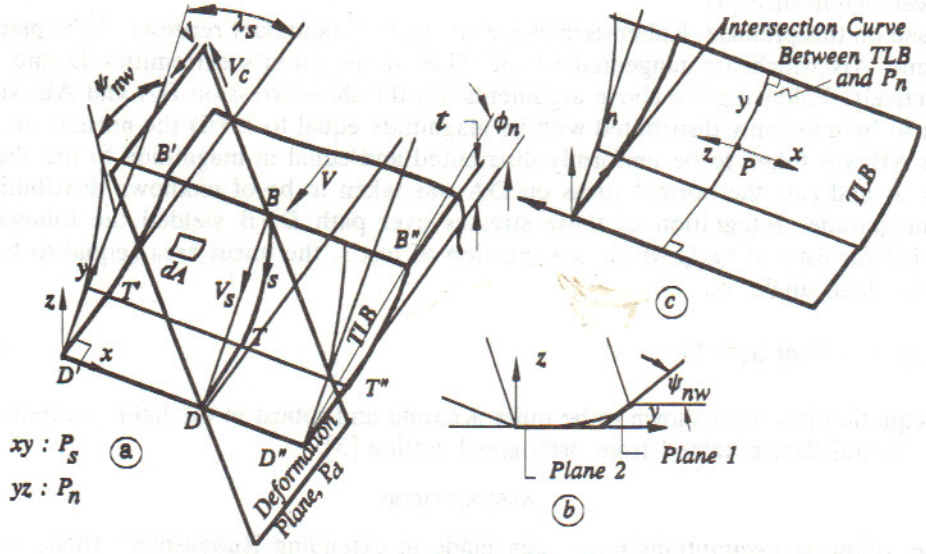

Fig. 3. The lower boundary of the shear zone in single edge oblique cutting.

the normal force on dA. Following assumption A7, the shear stress is assumed to be directed along the curved line of intersection of the deformation plane, P_d, with the area element. Thus the shear force vector on dA is given by $s\ (dA)\{(\mathbf{u}_{ndA} \times \mathbf{u}_{nd})/\sin\xi_{dA})\}$, where $\mathbf{u}_{nd}$ is the unit vector normal to P_d, "$\times$" represents the vector product operation and ξ_{dA} is the acute angle between $\mathbf{u}_{nd}$ and $\mathbf{u}_{ndA}$. Note that ξ_{dA} is equal to $\arccos(\mathbf{u}_{ndA} \cdot \mathbf{u}_{nd})$ where "$\cdot$" represents the scalar product operation. It is now desired to find the contribution, df_j, due to the normal and shear forces acting on dA, to the total cutting force component, f_j, in the direction of an arbitrary unit direction vector, $\mathbf{u}_j$. Clearly df_j can be expressed as

$$\begin{aligned} df_j &= \{s(dA)(\mathbf{u}_{ndA} \times \mathbf{u}_{nd})/\sin\xi_{dA}\} \cdot \mathbf{u}_j + p_{dA}\,(dA)\mathbf{u}_{ndA} \cdot \mathbf{u}_j \\ &= [s\{(d\mathbf{A} \times \mathbf{u}_{nd})/\sin\xi_{dA}\} + p_{dA}\,d\mathbf{A}] \cdot \mathbf{u}_j\,, \end{aligned} \tag{2}$$

where $d\mathbf{A}$ is the area vector of area element dA.

The total force f_j may be obtained by integrating df_j over the entire area of the TLB, so that

$$f_j = \left[\int_{TLB} \{s(d\mathbf{A} \times \mathbf{u}_{nd})/\sin\xi_{dA}\} + p_{dA}\,d\mathbf{A}\}\right] \cdot \mathbf{u}_j\,. \tag{3}$$

Note that in order to predict f_j from equation (3) we need to have *a priori* knowledge of the geometry of and the stress distribution on the TLB in addition to the orientations of vectors $\mathbf{u}_{nd}$ and $d\mathbf{A}$. In the next section, classical plasticity theory will be applied to the problem with a view to obtaining as much information concerning the stress distributions on the TLB as possible.

5. APPROXIMATE DETERMINATION OF THE STRESS DISTRIBUTIONS ON THE TLB

Consider a cubic infinitesimal volume of material at an arbitrary point P on the TLB [see Fig. 3(c)]. The Cartesian axes at point P are such that axis x is parallel to the cutting edge, axis y is tangential to the TLB at P and lies in the normal plane, and axis z is directed normal to the TLB at point P. Let ψ_n be the angle between the plane tangent to the TLB at P and the cutting plane, P_s. Let η_s be the angular deviation of the shear velocity at point P from the normal plane, P_n, when measured in the plane tangential to the TLB at point P. Now, following assumption A2 and applying classical plasticity theory, the following equations relating the normal stresses (σ values), shear stresses (τ values), velocities (V values) and strain rates ($\dot{\epsilon}$ values) can be written as:

$$\frac{\tau_{xy}}{\dot{\epsilon}_{xy}} = \frac{\tau_{yz}}{\dot{\epsilon}_{yz}} = \frac{\tau_{xz}}{\dot{\epsilon}_{xz}} = \frac{(\sigma_x - \sigma_m)}{\dot{\epsilon}_x} = \frac{(\sigma_y - \sigma_m)}{\dot{\epsilon}_y} = \frac{(\sigma_z - \sigma_m)}{\dot{\epsilon}_z}\,, \tag{4}$$

where

$$\sigma_m = \frac{1}{3}(\sigma_x + \sigma_y + \sigma_z) \tag{5a}$$

$$\dot{\epsilon}_x = \frac{\partial V_x}{\partial x} \tag{5b}$$

$$\dot{\epsilon}_y = \frac{\partial V_y}{\partial y} \tag{5c}$$

$$\dot{\epsilon}_z = \frac{\partial V_z}{\partial z} \tag{5d}$$

$$\dot{\epsilon}_{xy} = \frac{1}{2}\left(\frac{\partial V_x}{\partial y} + \frac{\partial V_y}{\partial x}\right) \tag{5e}$$

$$\dot{\epsilon}_{yz} = \frac{1}{2}\left(\frac{\partial V_y}{\partial z} + \frac{\partial V_z}{\partial y}\right) \tag{5f}$$

$$\dot{\epsilon}_{xz} = \frac{1}{2}\left(\frac{\partial V_z}{\partial x} + \frac{\partial V_x}{\partial z}\right). \tag{5g}$$

From assumption A5, it follows that velocity gradients ($\partial V_x/\partial x$, $\partial V_y/\partial x$ and $\partial V_z/\partial x$) along direction x, which is parallel to the cutting edge, must have zero magnitudes. Further, since the point under consideration is on the TLB which must be a "shear surface", the velocity gradient $\partial V_z/\partial y$ must also have zero magnitude. Thus

$$\frac{\partial V_x}{\partial x} = \frac{\partial V_y}{\partial x} = \frac{\partial V_z}{\partial x} = \frac{\partial V_z}{\partial y} = 0. \tag{6}$$

The assumption of thin shear zone (assumption A6) implies that the velocity gradients across the thickness of the zone (i.e. along z) must be substantially larger than those along its length (i.e. along y). Thus

$$\frac{\partial V_x}{\partial y}, \frac{\partial V_y}{\partial y} \ll \frac{\partial V_x}{\partial z}, \frac{\partial V_y}{\partial z} \tag{7}$$

so that it may be assumed that $\partial Vx/\partial y \approx \partial Vy/\partial y \approx 0$. Combining this observation with equations (5a), (5b), (5e)–(5g) and (6) yields

$$\dot{\epsilon}_x = 0 \tag{8a}$$

$$\dot{\epsilon}_y \approx 0 \tag{8b}$$

$$\dot{\epsilon}_{xy} \approx 0 \tag{8c}$$

$$\dot{\epsilon}_{yz} = \frac{1}{2}\frac{\partial V_y}{\partial z} \tag{8d}$$

$$\dot{\epsilon}_{xz} = \frac{1}{2}\frac{\partial V_x}{\partial z}. \tag{8e}$$

Next, combining equations (4a), (4c), (4d), (5a) and 8(a)–(8c) gives

$$\sigma_x \approx \sigma_y \approx \alpha_z \approx \sigma_m \tag{9a}$$

$$\tau_{xy} \approx 0. \tag{9b}$$

Following again the thin shear zone assumption, it may further be assumed that strain rates ($\dot{\epsilon}_{xz}$, $\dot{\epsilon}_{yz}$) are uniformly distributed across the thickness, Δz, of the shear zone. Hence these can be expressed in terms of the known work velocity, $\mathbf{V}$, and chip velocity, $\mathbf{V}_c$, as

$$\dot{\epsilon}_{xz} \approx \frac{1}{2}\left(\frac{V\sin\lambda_s - V_c\sin\eta_c}{\Delta z}\right) \tag{10a}$$

$$\dot{\epsilon}_{yz} \approx \frac{1}{2}\left(\frac{V\cos\lambda_s\cos\psi_n + V_c\cos\eta_c\sin(\psi_n - \gamma_n)}{\Delta z}\right). \tag{10b}$$

From the definition of η_s and combining equations (4), (10a) and (10b),

$$\tan\eta_s = \frac{V\sin\lambda_s - V_c\sin\eta_c}{V\cos\lambda_s\cos\psi_n + V_c\cos\eta_c\sin(\psi_n - \gamma_n)} \approx \frac{\dot{\epsilon}_{xz}}{\dot{\epsilon}_{yz}} \approx \frac{\tau_{xz}}{\tau_{yz}}. \tag{11}$$

Equation (11) implies that, at any point on the TLB, the shear stress and the shear velocity are approximately collinear. Now we substitute equations (9a) and (9b) into van Mises yield condition

$$(\sigma_z - \sigma_m)^2 + (\sigma_z - \sigma_m)^2 + (\sigma_z - \sigma_m)^2 + 6(\tau_{xy}^2 + \tau_{xy}^2 + \tau_{xy}^2) = 6s^2 \tag{12}$$

(where s is the flow stress of the unmachined work material) to obtain

$$\tau_{xz}^2 + \tau_{yz}^2 \approx s^2 . \tag{13}$$

Combining equation (13) with equation (11), it is noted that

$$\tau_{yz} \approx s \cos \eta_s \tag{14a}$$

$$\tau_{xz} \approx s \sin \eta_s . \tag{14b}$$

Now, the following equations for the shear and normal stresses, $\tau_{y\theta}$ and σ_θ, respectively, on a plane perpendicular to the yz plane and inclined at angle θ to plane xy (which is tangential to TLB) can be obtained from the equilibrium condition (see Fig. 4):

$$\tau_{y\theta} \cos\theta - \sigma_\theta \sin\theta + \sigma_y \sin\theta + \tau_{yz} \cos\theta = 0 \tag{15a}$$

$$\sigma_z \cos\theta + \tau_{yz} \sin\theta - \sigma_\theta \cos\theta - \tau_{y\theta} \sin\theta = 0 . \tag{15b}$$

However, we know that the normal stress is of zero magnitude on the surface of the unmachined work material. Likewise, following assumption A5, it may be assumed that the shear stress in the plane, P_n, normal to the tool cutting edge, is also of zero magnitude. Thus, letting $\theta = \psi_{nw}$ and $\tau_{y\theta} = \sigma_\theta = 0$ (where ψ_{nw} is the magnitude of ψ_n at the junction between the TLB and the unmachined work surface) in equations (15a) and (15b), gives

$$\sigma_z \approx -\tau_{yz} \tan\psi_{nw} \tag{16a}$$

$$\sigma_y \approx -\tau_{yz} \cot\psi_{nw} ; \tag{16b}$$

but from equation (9a), $\sigma_z \approx \sigma_y$, so that

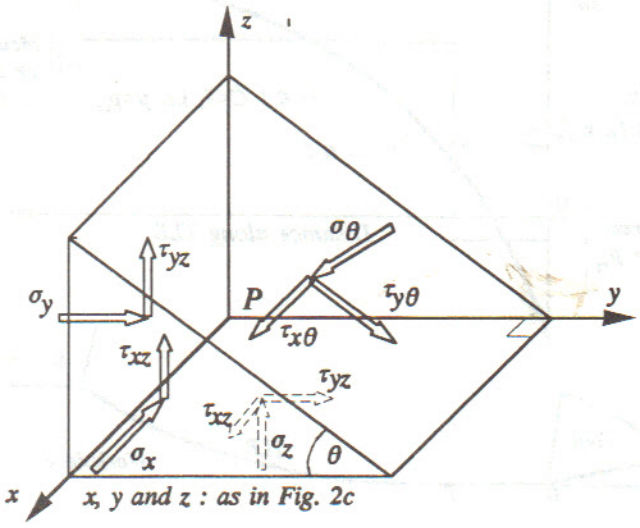

Fig. 4. Stresses on a plane perpendicular to the yz plane at a point P on the TLB.

$$\psi c_{nw} \approx 45^\circ . \tag{17}$$

Equation (17) implies that, in oblique cutting, the TLB meets the unmachined work surface at an angle *approximately* equal to 45° (whereas, in orthogonal cutting, it meets exactly at an angle of 45° [4]).

Finally, it follows from equations (14a), (14b), (16) and (17) that the magnitude of the normal stress, p_w, on the TLB where it meets the unmachined work surface is given by

$$p_B \approx \sigma_z \text{ at } B \approx \tau_{yz} \tan\psi_{nw} \approx \tau_{yz} \approx s \cos \eta_{sw} , \tag{18}$$

where η_{sw} is the magnitude of η_s at the junction between the TLB and the unmachined work surface (we will identify the method of estimating η_{sw} later).

Now, as in [4], it could be assumed that the normal stress on the portion B′B″T″T, which is not coincident with the cutting plane, is uniformly distributed so that the magnitude of p_{dA} in equation (3) can be taken to be equal to $s \cos \eta_{sw}$, at least over the non-coincident portion of the TLB (see curve b in Fig. 3). However, there is considerable evidence in orthogonal cutting literature that the stresses in the shear zone in the vicinity of the cutting edge are tensile, whereas they are compressive elsewhere in the zone. Thus, one can expect that the actual normal stress distribution on the lower boundary is of the form characterized by curve a in Fig. 5. If this is the case, the mean normal stress, p, on the non-coincident segment (BT in Fig. 2, or B′B″T″T′ in Fig. 3) of the TLB should be smaller than the normal stress at the junction, B, with the unmachined surface, i.e. the magnitude of p should be a fraction C of the normal stress at B so that

$$p = C s \cos \eta_{sw} . \tag{19}$$

6. PREDICTION OF FORCE COMPONENTS PARALLEL TO THE CUTTING PLANE, P_s

The ideal method of estimating f_j is to use equation (3) and perform the integration involved in it over the TLB. However, since the complete geometry of the TLB is unknown, the possibility of using an assumed path of integration was investigated. In

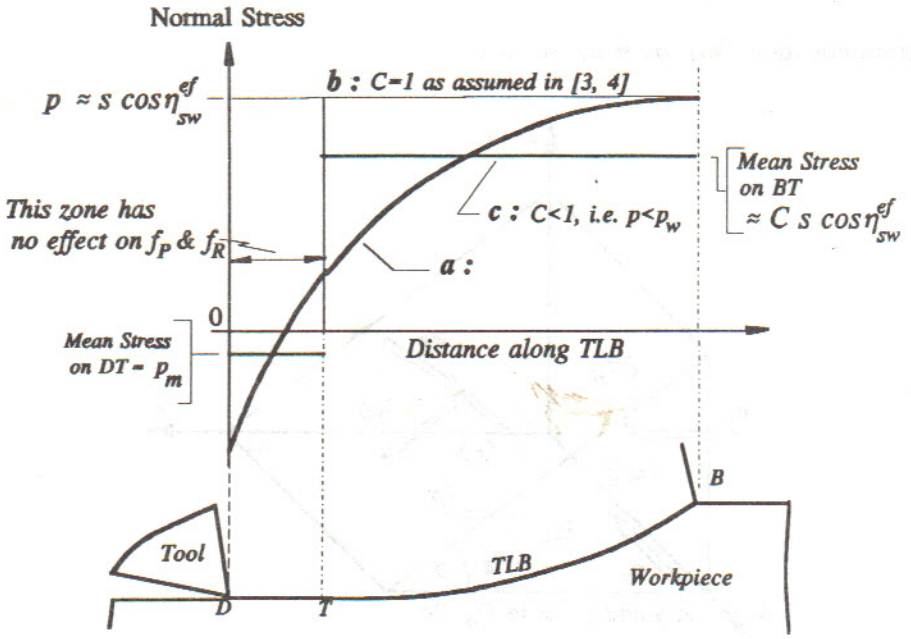

Fig. 5. Idealization of the normal stress distribution on the lower boundary of the shear zone.

particular, a path consisting of two planes, namely planes 1 and 2, similar to the method adopted in orthgonal cutting [4] as illustrated in Fig. 3(b) was considered. Here, plane 1 is inclined to the cutting plane, P_s, at an arbitrary angle ψ_{n1}, whereas plane 2 is parallel to P_s. In order to enable force estimation from such an assumed path, equation (3) can be rewritten as

$$f_j = \left[\sum_{i=1}^{2} \{s(\mathbf{A}_i \times \mathbf{u}_{nd})/\sin \xi_i + p_i \mathbf{A}_i\}\right] \cdot \mathbf{u}_j$$

$$= s\{(\mathbf{A}_1 \times \mathbf{u}_{nd})/\sin \xi_1 + C \cos \eta_{sw1} \mathbf{A}_1\} \cdot \mathbf{u}_j + s\{(\mathbf{A}_2 \times \mathbf{u}_{nd})/\sin \xi_2 + p_m \mathbf{A}_2\} \cdot \mathbf{u}_j), \quad (20)$$

where $\mathbf{A}_1$ and $\mathbf{A}_2$ are the area vectors of planes 1 and 2 in the assumed path of integration, η_{sw1} is the magnitude of as evaluated for plane 1, p_1 and p_2 are the mean normal stresses on planes 1 and 2, respectively, given by $p_1 = C\, s \cos\eta_{sw1}$ and $p_2 = p_m$ (of unknown magnitude), and ξ_1 and ξ_2 are the acute angles between vectors $\mathbf{A}_1$ and $\mathbf{u}_{nd}$, and between $\mathbf{A}_2$ and $\mathbf{u}_{nd}$, respectively.

Note that equation (20) contains the parameter p_m of unknown magnitude. However, if the prediction is confined to a force component (such as f_{ed}, f_{Pn}, f_R, or f_P) parallel to the cutting plane, P_s, the term $\mathbf{A}_2 \cdot \mathbf{u}_j$ will clearly vanish (since in this case $\mathbf{A}_2$ is perpendicular to plane P_s where $\mathbf{u}_j$ is parallel to plane P_s). Thus

$$f_j = s\{(\mathbf{A}_1 \times \mathbf{u}_{nd})/\sin \xi_1 + (\mathbf{A}_2 \times \mathbf{u}_{nd})/\sin \xi_2 + C \cos \eta_{sw1} \mathbf{A}_1\} \cdot \mathbf{u}_j \quad (21)$$

provided that the condition $\mathbf{u}_j \| P_s$ is satisfied.

The presence of $\mathbf{u}_{nd}$ in the above equation implies that f_j depends on the orientation of the deformation plane, P_d. Further, the presence of terms $\sin \xi_1$ and $\sin \xi_2$ in the equation implies that the resulting f_j estimate is path dependent, i.e. the estimate of f_j will depend on the assumed geometry of the lower boundary of the shear zone. In fact, it can be demonstrated that there is no deformation plane passing through $\mathbf{V}_s$ which results in the $\sin \xi_1$ and $\sin \xi_2$ terms vanishing from equation (21). It is therefore concluded that assumption A7 prevents the finding of a path-independent solution to oblique cutting. In contrast, if the assumption that deformation could occur over a curved surface (still passing through $\mathbf{V}_s$) is allowed, it might be possible to arrive at a path-independent solution to the problem. However, such an analysis would require knowledge of the exact geometry of the TLB. Since the exact geometry of the TLB is unknown, the feasibility of finding an approximately path-independent solution to the problem may now be examined. In particular, a plausible deformation plane will be defined which appears to lead to a path dependency within acceptable limits. (It may be noted that Venuvinod and Lau had arbitrarily assumed in [5] that P_d was normal to P_s.)

The "effective plane", P_{ef}, is now proposed as a candidate for the deformation plane P_d (recall assumption A7), i.e. $P_d \equiv P_{ef}$. This proposal is inspired by the observation that several previous investigators (in particular Shaw [2]) have found that the concept of the effective plane is capable of accounting for several commonly observed phenomena in single edge oblique cutting. Shaw [2] defined the effective plane, P_{ef}, as the plane parallel to the initial work velocity, $\mathbf{V}$, as well as the final chip velocity, $\mathbf{V}_c$. Note that, since $\mathbf{V}_s = \mathbf{V} - \mathbf{V}_c$, this definition implies that P_{ef} is also parallel to $\mathbf{V}_s$.

Thus, provided that the condition $\mathbf{u}_j \| P_s$ is satisfied, equation (21) can be rewritten as follows by replacing $\mathbf{u}_{nd}$ with the unit vector, $\mathbf{u}_{nef}$, normal to P_{ef},

$$f_j = s[\{(\mathbf{A}_1/\sin \xi_1) + (\mathbf{A}_2/\sin \xi_2)\} \times \mathbf{u}_{nef} + C \cos \eta_{sw1}^{ef} \mathbf{A}_1] \cdot \mathbf{u}_j, \quad (22)$$

where η_{sw1}^{ef} is the magnitude of η_{sw1} when P_d is taken parallel to P_{ef}; ξ_1 and ξ_2 are redefined as the acute angles between $\mathbf{A}_1$ and $\mathbf{u}_{nef}$, and, $\mathbf{A}_2$ and $\mathbf{u}_{nef}$, respectively.

Equation (22) can be further simplified by noting and incorporating the following observations derived from the geometry of chip formation in oblique cutting.

(1) The area of Merchant shear plane, A_m, is given by

$$A_m = bt/(\cos\lambda_s \sin\phi_n) . \tag{23}$$

(2) Since the bounding edges of the chain of planes, 1 and 2, used in approximating the TLB is common with those of the Merchant shear plane,

$$\mathbf{A}_1 + \mathbf{A}_2 = \mathbf{A}_m = \mathbf{A}_m \mathbf{u}_m , \tag{24}$$

where $\mathbf{u}_m$ is the unit vector normal to the Merchant shear plane, P_m. (This is in fact true whatever the chain of planes used to approximate the TLB.)

(3) We arbitrarily assume that (we shall evaluate the error resulting from this assumption later)

$$\mathbf{A}_1/\sin\xi_1 + \mathbf{A}_2/\sin\xi_2 \approx \mathbf{A}_m/\sin\xi_m . \tag{25}$$

(4) From the definition of P_{ef} and the relative orientations of P_{ef} and P_m, we note that

$$(\mathbf{A}_m \times \mathbf{u}_{nef})/\sin\xi_m = A_m(\mathbf{u}_m \times \mathbf{u}_{nef})/\sin\xi_m = A_m \mathbf{u}_{V_s} , \tag{26}$$

where $\mathbf{u}_{V_s}$ is the unit vector in the direction of the shear velocity vector, $\mathbf{V}_s$, on the Merchant shear plane and ξ_m is the angle between $\mathbf{u}_m$ and $\mathbf{u}_{nef}$.

(5) Equation (17) states that plane 1 meets the unmachined work surface at an angle of 45°. Thus it can be shown, by replacing η_{sw1}^{ef} by η_{sw}^{ef} in equation (22) and taking $\psi_n = 45°$ in equation (11), that

$$\eta_{sw}^{ef} = \arctan[\{\tan\lambda_s \cos(45° - \gamma_n) - \tan\eta_c \sin 45°\}/\cos\gamma_n] . \tag{27}$$

(6) Since $\mathbf{A}_2$ is normal to P_s and $\mathbf{A}_2 \cdot \mathbf{u}_j = 0$ when $(\mathbf{u}_j \| P_s)$, the following vector transformations can be made:

$$C\cos\eta_{sw}^{ef}\,\mathbf{A}_1 \cdot \mathbf{u}_j = C\cos\eta_{sw}^{ef}\,(\mathbf{A}_1 + \mathbf{A}_2) \cdot \mathbf{u}_j = C\cos\eta_{sw}^{ef}\,(\mathbf{A}_m \cdot \mathbf{u}_j) . \tag{28}$$

Now combining equations (22)–(28), it can be shown that

$$f_j \approx sA_m\{(\mathbf{u}_{V_s} \cdot \mathbf{u}_j) + C\cos\eta_{sw}^{cf}\,(\mathbf{u}_{V_s} \cdot \mathbf{u}_j)\} \tag{29}$$

provided that the condition $\mathbf{u}_j \| P_s$ is satisfied.

Equation (22) is a path-dependent version that will yield an exact solution to the problem of estimating f_j, provided that the assumed path of the lower boundary (LB) corresponds to that of the true LB. In contrast, equation (29) is an approximate but path-independent solution.

It is believed that the TLB, in practice, would lie somewhere between two extremes. One extreme is the case when the TLB is identical to the Merchant shear plane except for the fact that the TLB moves away from the Merchant shear plane in the vicinity of its junction with the unmachined work surface so as to satisfy the condition that $\psi_{nw} = 45°$. In such a situation, equation (29) yields the exact solution. The other extreme occurs when the geometry of the TLB is such that it can be approximated by two planes, of areas A_1 and A_2 as described in the derivation of equation (22), but with the condition that the LB segment with area A_1 is inclined at angle 45° to P_s.

The f_j estimate in this case can be obtained from equation (22) with suitably substituted parameters.

The difference between the f_j estimates obtained in the above two extreme solutions represents the maximum error associated with the use of equation (29). This error can be expressed as a percentage of the estimate obtained from equation (29). When such a procedure was applied to the empirical data reported in [6] for machining aluminium alloy with single edge oblique tools, it was found that percentage errors associated with equation (29) were within ± 3% even when λ_s was as large as 50°. For practical purposes, this is believed to be an acceptable range of error.

Now taking $\mathbf{u}_j$ in equation (29) to be successively parallel to f_{ed}, f_{Pn}, f_R and f_P and evaluating the corresponding scalar products in terms of the geometric data set $\{\lambda_s, \phi_n, \eta_c\}$ it can be shown that

$$f_{ed} \approx sA_m \sin \eta_{sm} \tag{30}$$

$$f_{Pn} \approx sA_m (\cos \eta_{sm} \cos \phi_n + C \cos \eta_{sw}^{ef} \sin \phi_n) \tag{31}$$

$$f_R = sA_m (\cos \eta_{sm} \cos \phi_n \sin \lambda_s - \sin \eta_{sm} \cos \lambda_s + C \cos \eta_{sw}^{ef} \sin \phi_n \sin \lambda_s) \tag{32}$$

$$f_P \approx sA_m (\cos \phi_e + C \cos \eta_{sw}^{ef} \sin \phi_n \cos \lambda_s) , \tag{33}$$

where ϕ_e, the effective shear angle, is given by

$$\phi_e = \arccos(\cos \eta_{sm} \cos \phi_n \cos \lambda_s + \sin \eta_{sm} \sin \lambda_s) \tag{34}$$

and η_{sm} is given by

$$\eta_{sm} = \arctan[\{\tan \lambda_s \cos(\phi_n - \gamma_n) - \tan \eta_c \sin \phi_n\}/\cos \gamma_n] . \tag{35}$$

Note, when $\lambda_s = 0$ (and therefore $\eta_c = 0$) and $C = 1$, equation (33) reduces to the corresponding equation for orthogonal cutting [see equation (1)]. Thus, Rubenstein's solution to orthogonal cutting [4] is a specific case of the solution to oblique cutting developed here.

7. ESTIMATION OF THE THRUST FORCE COMPONENT, f_Q

Equation (3) does not facilitate the estimation of the thrust force component, f_Q, because of the unknown magnitude of p_m which acts in the direction of f_Q. However, assuming that the Principle of Force–Velocity Collinearity is obeyed at the chip–tool interface, it is possible to derive the following equation for estimating f_Q from the previously estimated magnitudes of f_{ed} and f_{Pn} [see equations (30) and (31)] which are not influenced by p_m (this condition and the following equation are implicit in the oblique cutting analyses described in [1, 2, 5,6]):

$$f_Q = \{f_{ed}/(\tan \eta_c \cos \gamma_n)\} - f_{Pn} \tan \gamma_n . \tag{36}$$

8. EXPERIMENTAL VERIFICATION OF THE NEW MODEL AND DISCUSSION

The force predictions resulting from the above model against experimental data were then tested. In particular, data on single edge oblique cutting of an aluminium alloy, copper and mild steel presented in [6] and further experimental data (reproduced in Table 1) obtained by the author while cutting another aluminium alloy were used. The experimental procedure used in the further experiments was identical to that adopted in [6]. Chip thicknesses, chip flow angles and cutting forces were measured while dry cutting with a range of tool geometries and uncut-chip thicknesses (λ_s = 0–50°, γ_n = 25 and 30°, t = 0.05–0.175 mm). Edge forcces were removed from the measured force components by the method used in [6] to yield the magnitudes of f_P, f_Q, and f_R arising

Table 1. New oblique cutting data: machining aluminium alloy†

		Normal rake, $\gamma_n = 25°$					Normal rake, $\gamma_n = 30°$				
t (mm)	λ_s (deg)	ϕ_n (deg)	η_c (deg)	f_P (N)	f_R (N)	f_Q (N)	ϕ_n (deg)	η_c (deg)	f_P (N)	f_R (N)	f_Q (N)
0.050	0	31.4	0	169	0	29	35.5	0	174	0	19
0.075	0	32.0	0	269	0	49	35.5	0	254	0	29
0.100	0	34.0	0	329	0	54	35.5	0	334	0	39
0.125	0	33.0	0	429	0	74	35.5	0	424	0	49
0.150	0	33.0	0	519	0	89	35.5	0	494	0	54
0.175	0	35.1	0	599	0	104	35.5	0	604	0	69
0.050	10	32.0	10	193	16	20	35.5	11	145	20	16
0.075	10	35.1	10	263	26	45	35.5	12	245	30	27
0.100	10	33.0	10	343	26	60	36.6	11	320	40	37
0.125	10	34.0	9	463	36	80	36.6	11	420	50	47
0.150	10	34.0	9	543	46	85	37.7	10	460	60	52
0.175	10	35.1	10	633	56	90	37.7	10	550	70	62
0.050	20	33.0	18	166	53	17	37.7	18	183	38	22
0.075	20	34.0	20	236	68	27	37.7	20	253	53	34
0.100	20	35.1	20	336	88	37	37.7	16	338	88	44
0.125	20	35.1	24	436	108	52	38.8	20	418	88	52
0.150	20	35.1	16	506	138	57	38.8	19	498	103	64
0.175	20	35.1	21	566	168	62	38.2	18	618	128	79
0.050	30	34.0	30	191	55	29	37.7	30	141	50	9
0.075	30	35.1	30	261	75	44	37.7	33	236	67	21
0.100	30	36.1	32	341	95	59	37.7	28	316	92	23
0.125	30	37.1	34	401	115	69	37.7	27	386	117	26
0.150	30	38.1	36	521	150	84	37.7	27	446	137	31
0.175	30	37.1	34	631	180	104	37.7	29	536	167	41
0.050	40	35.1	35	217	87	21	37.7	40	151	63	4
0.075	40	36.1	36	297	122	41	38.8	38	276	116	14
0.100	40	37.1	44	407	152	66	38.8	36	361	151	14
0.125	40	37.1	37	497	192	66	38.8	36	436	173	19
0.150	40	38.1	36	647	242	106	38.8	39	521	218	21
0.175	40	38.1	37	707	287	81	38.8	36	596	248	24
0.050	50	37.1	45	164	75	2	40.9	46	195	106	−4
0.075	50	38.1	51	299	190	12	40.9	46	220	116	−1
0.100	50	39.1	48	299	190	12	39.8	52	350	176	−1
0.125	50	40.1	46	444	270	7	39.8	47	400	211	−1
0.150	50	40.1	50	529	310	17	40.9	47	500	261	−6
0.175	50	41.0	44	659	375	17	40.9	47	605	321	−6

†HSS tool, dry cutting, work width 6 mm.

from chip formation. The shear angles were estimated from the chip length ratios since these exhibited smaller scatter than those estimated from chip thickness ratios.

On preliminary analysis, none of the above data sets was found to satisfy the condition of collinearity between $\mathbf{V}_c$ and the friction force at the chip–tool interface. Hence, no attempt was made to test the prediction of f_Q from equation (36) and the discussion will be confined to testing the prediction of force components parallel to the cutting plane, P_s.

However, irrespective of the validity of the Principle of Force–Velocity Collinearity at the chip–tool interface, equations (32) and (33) can be used to compute the predicted f_R and f_P, respectively. These predicted magnitudes can then be compared with the corresponding measured magnitudes of f_R and f_P, respectively, with a view to verifying the new oblique cutting model.

8.1. *Estimation of* s *and* C *for a given work material*

The prediction of f_R and f_P from equations (32) and (33) requires *a priori* knowledge of parameters s and C. It has already been argued that s must be a material constant since it is the shear flow strength of the unmachined work material. In contrast, C

characterizes the degree of non-uniformity of the normal stress on the TLB. A larger deviation of C from unit magnitude implies a larger degree of non-uniformity of the normal stress distribution on the non-coincident portion of TLB. Further, it is not immediately clear whether C is a material constant. A review of orthogonal cutting literature suggests that the normal stress distribution in the shear zone could depend on the work material and the rake angle. It is now hypothesized that C is strongly dependent on the work material, only weakly dependent on the rake angle, and independent of other cutting conditions (such as t). (Empirical evidence in support of this hypothesis will be examined later.)

It is intended to be able to predict any force component parallel to P_s. To enable this, s and C need to be estimated using equations (30) and (31), respectively. Equation (30) suggests that s can be estimated independently of C by examining the correlation between the predicted magnitudes of f_{ed}/s and the corresponding measured magnitudes of f_{ed}. In contrast, the use of equation (31) for predicting f_{Pn} involves s and C simultaneously. However, a preliminary analysis of experimental data shows that f_{ed} measurements usually exhibit greater scatter than f_{Pn} measurements. Hence, both equations (30) and (31) will be used in the estimation of s and C. Further, it may be noted that the estimation of s from equation (30) becomes indeterminate when applied to orthogonal cutting data (i.e. data obtained with $\lambda_s = 0$).

In view of the above observations, the following procedure was applied to data obtained with λ_s equal to 10, 30 and 50° for estimating the magnitudes of s and C for each work material.

(1) The magnitudes of f_{ed}/s and f_{Pn}/s were estimated from equations (30) and (31), respectively, for different magnitudes of C selected in the range 0–2. (2) For each value of C, a linear regression without intercept on the ordinate was performed by taking predicted f_{ed}/s and f_{Pn}/s values as abscissa values and the corresponding measured values f_{ed} and f_{cn} as ordinate values. The standard error and the coefficient of determination resulting from this regression exercise were noted.

(3) The magnitude of C resulting in the smallest standard error was taken as the best estimate of C. The slope of the regression line associated with the best C was taken as the best estimate of s.

Table 2 shows the results obtained by applying the above procedure to oblique cutting data taken from four different sources. It may be noted that each data set contains at least 18 readings obtained by varying t in the range 0.05–0.175 mm, and λ_s in the range 10–50°. Further, the coefficient of determination in every case was larger than 0.97. This validated the assumption that s and C were independent of t and λ_s. In addition, an application of a similar regression analysis to each of the data subsets in Table 1, corresponding to γ_n equal to 25 and 30°, showed that the best estimate of C was equal to 0.82 for both the data subsets. This indicated that C was only weakly dependent on γ_n. Together, these observations validated the assumption that s and C were work material constants.

Table 2. Results obtained from the application of the TLB model to experimental data†

Work material and cutting conditions	s (MPa)	C	Coefficient of determination	Data from reference
Aluminium alloy 1 $\gamma_n = 30°$	231.4	0.82	0.988	New data (Table 1)
Annealed aluminium alloy, HE9WP, $\gamma_n = 20°$	112.9	1.10	0.986	7
Commercially pure copper, $\gamma_n = 30°$	308.4	0.09	0.973	7
Annealed mild steel, $\gamma_n = 25$ and 30°	398.8	0.47	0.992	7

†HSS tool, dry cutting, $V = 3$ m/min.

Once the magnitudes of s and C were thus estimated from a limited set of oblique cutting data on a given work material, it became a straightforward exercise to predict f_R and f_P for any other oblique cutting condition from equations (32) and (33), respectively. Figure 6 illustrates the correlation between predicted and measured f_R and f_P for λ_s equal to 0, 20 and 40° (note that these are different from the λ_s values used for the parameter estimation) for the four work materials listed in Table 2. The large magnitude of coefficient of determination (equal to 0.975) obtained demonstrates successfully the ability of the new model in predicting at least two of the three cutting force components in single edge oblique cutting. Further, unlike the widely used Merchant shear plane model [1, 2], the new oblique cutting model has achieved this high degree of force prediction ability without requiring the invocation of the Principle of Force–Velocity Collinearity at the rake face and any *a priori* knowledge of the state of friction at the chip–tool interface.

However, when Fig. 6 was decomposed into data for f_R and f_P separately, it was noted that the coefficient of determination for f_R assumed the smaller value of 0.951, while that for f_P remained fairly high at 0.977 (see Table 2). This indicated that while f_R might not be predicted with great confidence, one can indeed do so with regard to f_P. This is fortunate from a practical point of view, since f_P is the power component of the cutting force.

Consider now the case of orthogonal cutting which is the condition obtained when $\lambda_s = 0$. In this case, $A_m = (b\,t)/\sin\phi_n$, $\phi_e = \phi_n$ and $\eta_{sw}^{cf} = 0$ so that equation (33) assumes the following simplified form:

$$f_P = sbt(\cot\phi_n + C)\,. \tag{37}$$

The above equation reduces to the original orthogonal cutting equation derived by Connolly and Rubenstein [3] if C is assumed to be equal to unity. Thus, the present oblique cutting model has enabled a refinement of Connolly and Rubenstein's model of orthogonal cutting [3] where it was arbitrarily assumed that the normal stress distribution on the "non-coincident" portion of the TLB was uniform, i.e. $C = 1$. This was necessary because the problem of orthogonal cutting could not be solved otherwise. However, the present work has shown that this assumption is not necessary if s and C are estimated from oblique cutting data.

Moreover, a detailed analysis of the regression results obtained during the parameter estimation exercises showed that the standard error associated with the estimation of

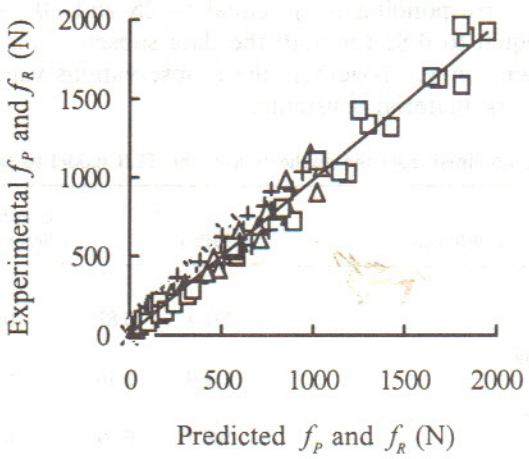

Fig. 6. Correlation between predicted and measured magnitudes of f_P and f_R (×) Al, $\gamma_n = 25°$, and 30°, Table 1; (+) Al, $\gamma_n = 30°$, [7]; (△) copper, $\gamma_n = 30°$, [7]; (□) mild steel, $\gamma_n = 20°$ [7]. $\lambda_s = 0$, 20 and 40°, $t = 0.05$–0.175 mm, HSS tool, dry cutting. Slope of regression line = 1.001. Coefficient of determination = 0.975.

s was quite insensitive to even substantial variations in C in the vicinity of the best estimate of C. For instance, in cutting the aluminium alloy [7], the variation in standard error was found to be less than 2% even when C was varied in the range 0.8–1.4. A similar situation was noted when the data in Table 1 (while cutting another aluminium alloy) were analysed. It was therefore concluded that, at least in the case of cutting aluminium alloys, it may be assumed that C is approximately equal to unity.

9. CONCLUSION

A new analysis of single edge oblique cutting based on a model of the geometry of, and stress distributions on, the true lower boundary of the shear zone has been presented. Equation (29) may be used to predict any force component parallel to the cutting plane with reasonable accuracy solely from a knowledge of the flow stress, s, of the work material, the uncut area, the shear angle, and the chip flow angle. The application of the model does not require any *a priori* knowledge of the friction conditions prevailing at the chip–tool interface. Thus, the model is an improvement over previous models based on the Merchant shear plane [1, 2] which, although widely used, do not have the ability to predict any of the cutting force components without *a priori* knowledge of the state of friction at the chip–tool interface. Further, the thrust force component, f_Q, can be predicted provided the Principle of Force–Velocity Collinearity between the tangential force is satisfied at the tool–chip interface. It turns out, however, that such collinearity is rarely observed in empirical data on oblique cutting. Further research is needed to resolve this problem.

The new model has demonstrated a rigorous and direct approach to the modelling of the stress distributions on the lower boundary of the shear zone in oblique cutting. However, the model is unable to achieve an exact and path-independent solution to oblique cutting. The present work has demonstrated that it is important to recognize the significance of the non-uniformity of the normal stress distribution on the TLB. This aspect was left unaddressed in the original orthogonal cutting model [3, 4] of Rubenstein. Further research is needed to investigate the full implications of this observation.

Acknowledgements—The author thanks the City University of Hong Kong for the financial support (Strategic Research Grant 781) provided for this work. Further, the work of Mr C. M. Lee, Research Assistant, in collecting the new oblique cutting data presented in Table 1 is acknowledged.

REFERENCES

[1] M. E. Merchant, *J. Appl. Mech.* **66,** A168 (1944).
[2] M. C. Shaw, *Metal Cutting Principles,* 3rd edition. M.I.T. Press, Cambridge, Massachusetts (1957).
[3] R. Connolly and C. Rubenstein, *Int. J. Mach. Tool Des. Res.* **8,** 159 (1968).
[4] C. Rubenstein, *Int. J. Mach. Tool Des. Res.* **12,** 121 (1972).
[5] P. K. Venuvinod and W. S. Lau, *Trans. Am. Soc. Mech. Engrs J. Engng Ind.* **100,** 287 (1978).
[6] W. S. Lau and C. Rubenstein, *Int. J. Mach. Tool Des. Res.* **23,** 21 (1983).
[7] C. Rubenstein, *Int. J. Mach. Tool Des. Res.* **23,** 11 (1983).